ChemComm
Chemical Communications

This article can be cited before page numbers have been issued, to do this please use: K. I. Shivakumar, S. Noro, Y. Yamaguchi, Y. ISHIGAKI, A. Saeki, K. Takahashi, T. Nakamura and I. Hisaki, *Chem. Commun.*, 2021, DOI: 10.1039/D0CC07776C.

View Article Online
DOI: 10.1039/D0CC07776C

COMMUNICATION

Hydrogen-bonded organic framework based on redox-active tri(dithiolylidene)cyclohexanetrione

Received 00th January 20xx,
Accepted 00th January 20xx

DOI: 10.1039/x0xx00000x

Kilingaru I. Shivakumar,[a] Shin-ichiro Noro,[b] Yuna Yamaguchi,[c] Yusuke Ishigaki,[d] Akinori Saeki,[e] Kiyonori Takahashi,[a] Takayoshi Nakamura,*[a] and Ichiro Hisaki*[c]

Redox-active hexakis(4-carboxyphenyl) tri(dithiolylidene)-cyclohexanetrione (CPDC) was synthesized. The CPDC-based porous framework, constructed via anomalistic helical hydrogen-bonding, exhibited permanent porosity and photoconductivity.

Hydrogen-bonded organic frameworks (HOFs),[1-7] endowed with reversible intermolecular H-bonds and consequent high crystallinity, are new entrants to the family of crystalline porous materials.[8-10] Their unique features such as facile processability, self-healing, and regeneration make HOFs an attractive alternative to metal-organic frameworks (MOFs) and covalent organic frameworks (COFs).[1-7] These characteristics combined with their applications in selective sorption, catalysis, photoluminescence, and proton conduction underpin the growing interest in HOFs in recent years.[1-7]

A C_3- or C_6-symmetric, shape-persistent, hexatopic carboxylic acid derivative is one of the useful building blocks to construct stable HOFs with permanent porosity because they can form multiple intermolecular hydrogen bonds in well-defined and predictable manners.[3] We have earlier reported that C_3-symmetric planar π-conjugated hydrocarbons, such as triphenylene derivative **Tp**, forms a HOF with hexagonal network structures facilitated by a cyclic H-bonded motif,[11, 12] while hexaazatriphenylene derivative **CPHAT** forms a HOF with interpenetrated ***cpu***-networks via a helical H-bonding motif[13] (Fig. 1a).

In this study, we became interested in redox-active dithiolylidene-based C_3-symmetric core, tri(dithiolylidene)cyclohexanetrione (DC).[14] To date, C_2-symmetric X-shaped tetrathiafulvalene (TTF)-tetrabenzoic acid based HOF has been reported to furnish a simple 2D topology of rhombic networked (RhombNet) sheets, which stacked without interpenetration.[15] Recently, Xiao's group used the same molecule to obtain stable, H-bonded porous cocrystals that showed photocurrent response.[16] TTF based MOFs and COFs are also well-studied.[17] However, derivatives of DC are severely understudied, despite its first synthesis in 1980,[14] and certainly have not been used for the construction of porous frameworks, in spite of its fascinating properties such as amphoteric redox, solvatofluorochromism and charge conduction upon suitable substitution.[18, 19]

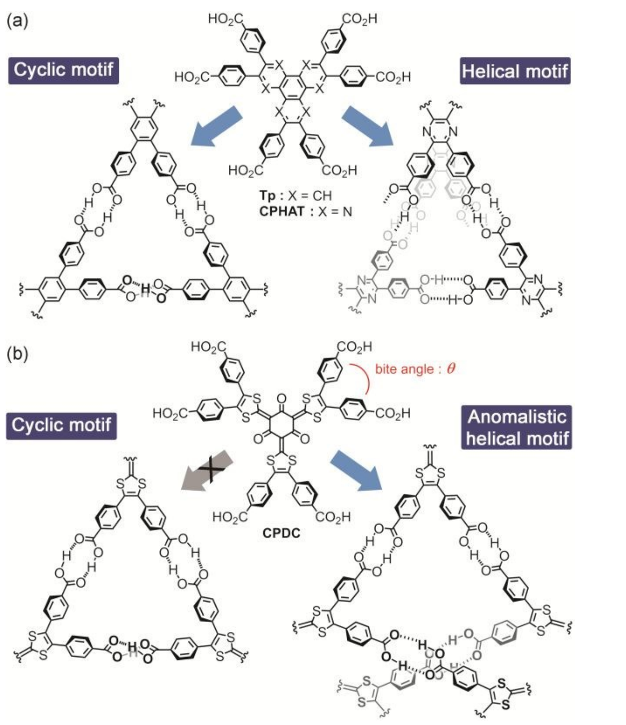

[a] Research Institute for Electronic Science, Hokkaido University, Sapporo, Hokkaido 001-0020, Japan.
[b] Faculty of Environmental Earth Science, Hokkaido University, Sapporo, Hokkaido 060-0810, Japan
[c] Graduate School of Engineering Science, Osaka University, 1-3 Machikaneyama, Toyonaka, Osaka 560-8531, Japan.
[d] Faculty of Science, Hokkaido University, Sapporo, Hokkaido 060-0810, Japan
[e] Graduate School of Engineering, Osaka University, 2-1 Yamadaoka, Suita, Osaka, 565 - 0871 Japan

† Electronic Supplementary Information (ESI) available: Synthesis, photophyics, electrochemistry, crystallography details and thermal analysis. CCDC-2038905 See DOI: 10.1039/x0xx00000x

View Article Online
DOI: 10.1039/D0CC07776C

Fig. 1 Hydrogen bonded motifs observed in HOFs of hexatopic building block molecules. (a) Cyclic and helical motif formed by **Tp** and **CPHAT**, respectively. (b) **CPDC** forming an anomalistic helical motif and not cyclic.

Herein, we report the first 3D-networked HOF of carboxyphenyl-substituted DC derivative, **CPDC**. Interestingly, the HOF **CPDC-1** is constructed through anomalistic helical H-bonded motif, instead of planar or simple helical motifs reported in the literature. This unusual H-bonding motif probably originates from slightly larger bite angle of **CPDC** (Fig. 1c), which can contribute to establish a rule of thumb for designing HOF. The synthesis of **CPDC**, preparation and crystallography of HOF **CPDC-1** along with its thermal, gas sorption and photoconductive behaviours are described. Also, the photophysical and electrochemical properties of an ester derivative of **CPDC** are studied.

CPDC was synthesized as shown in Scheme 1. The dibenzonitrile derivative **1**, obtained according to the literature procedure[20] from commercially available 1,3-dithiole-2-thione in two steps with overall yield of 37%, was hydrolysed in an acidic medium to obtain dibenzoic acid **2** in 54% yield. Fisher esterification of **2** resulted in dibenzoate ester **3** in 93% yield. The aromatic electrophilic substitution of phloroglucinol by **3**, mediated by triethylamine in presence of silver nitrate,[19] afforded the C_3-symmetric hexabenzoate **4** in 86% yield. The target compound **CPDC** was obtained by subjecting hexabenzoate **4** to saponification in 99% yield.

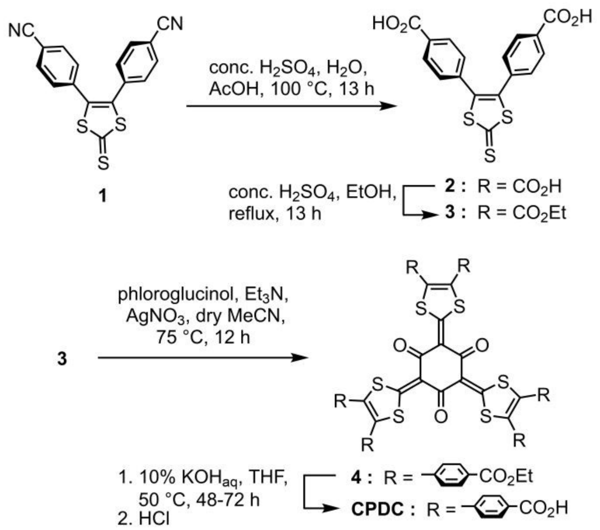

Scheme 1 Synthesis of **CPDC**.

The absorption spectrum of ester derivative **4** exhibits three prominent peaks at 246, 370, and 470 nm with the last showing maximum intensity (Fig. S8). The optical band gap obtained from the absorption edge of 488 nm was determined to be 2.54 eV. In order to obtain corresponding emission, the peak at 370 nm was chosen for excitation. The hexabenzoate **4** exhibited fluorescence with the intensity maximum at 491 nm with relative quantum yield (ϕ_F) of 0.76%. Differential pulse voltammetry (DPV) was performed to determine the redox behaviour of **4** as the cyclic voltammetry was less sensitive in distinguishing peaks (Fig. S9). The voltammogram shows multi-stage amphoteric redox behaviour with three prominent oxidation and three reduction peaks. The three sets of redox peaks plausibly suggest that all the three dithiole rings undergo sequential oxidation and reduction. The HOMO and LUMO energies were determined from the onset oxidation and reduction potentials and found to be −5.82 and -3.57 eV, respectively, affording an electrochemical band gap of 2.25 eV. Theoretical calculations carried out at B3LYP/6-31G** level on **CPDC** and a methyl ester of **CPDC** revealed stabilization of HOMO by electron-withdrawing carboxyl/carboxylate substituents (Figs. S11 and S12). The **CPDC** and its methyl ester possess the theoretical HOMO, LUMO and band gap energies of ca. 5.6-5.7, 2.2-2.3, and 3.35 eV, respectively (Table 1).

Table 1 Energy levels of molecular orbitals in **CPDC** and its esters.

Compound	E_{HOMO} (eV) [a]	E_{HOMO} (eV) [b]	E_{LUMO} (eV) [a]	E_{LUMO} (eV) [b]	E_g [a] (eV)	E_g [b] (eV)	E_g [c] (eV)
CPDC ester	-5.82	-5.57	-3.57	-2.21	2.25	3.35	2.54
CPDC	n.d.	-5.69	n.d.	-2.33	n.d.	3.36	n.d.

Determined from the [a]electrochemical experiment on **4**, [b]theoretical method applied to methyl ester of **CPDC**, and [c]absorption spectrum of **4**. E_g denotes band gap between HOMO and LUMO, and n.d. - not determined.

Slow evaporation of the solution of **CPDC** in a mixed solvent system consisting dimethylacetamide and methyl benzoate (MB) at 80 °C furnished orange needle-like solvated HOF crystals denoted as **CPDC-1**, in which all the six carboxylic acid groups participate in the formation of an H-bonded dimer. The **CPDC-1** crystallized in the space group of $C2/c$ and exhibits a porous framework constituted by hexagonally arranged **CPDC** molecules (Fig. 2a and Table S4). The ratio of total potential solvent area calculated from the PLATON software is 43% (cell volume: 7485.9 Å, void volume: 3219.4 Å). **CPDC** molecules are organized in an AB pattern with slipped π-stacking and stacked in a head-to-tail fashion with an intermolecular distance of 3.48 Å (Fig. 2b and 2c), while the four peripheral phenylene rings of **CPDC** are involved in parallel-displaced π-stacking, two each with layers above and below, by a shortest distance of 3.29 Å (Fig. S13a). The **CPDC** core is not strictly flat; nevertheless, has high planarity: the mean planes of dithiole rings deviate by 2.8–3.1° from mean plane of cyclohexanetrione and the root mean square deviation (RMSD) of the central DC core is 0.048 Å. Intramolecular S⋯O distances are 2.49–2.68 Å and are smaller than the sum of van der Waals (vdW) radii of the two atoms (Fig S13b). The two sulphur atoms in the dithioylidene rings form intermolecular S⋯S contacts at the distances of 3.77 and 4.00 Å. The former, although greater than sum of vdW radii of two sulphur atoms of 3.60 Å, is comparable to the intermolecular S⋯S contacts of 3.82 Å observed in conductive charge-transfer salt tetrathiafulvalene-tetracyanoquinodimethane (TTF-TCNQ).[21]

View Article Online
DOI: 10.1039/D0CC07776C

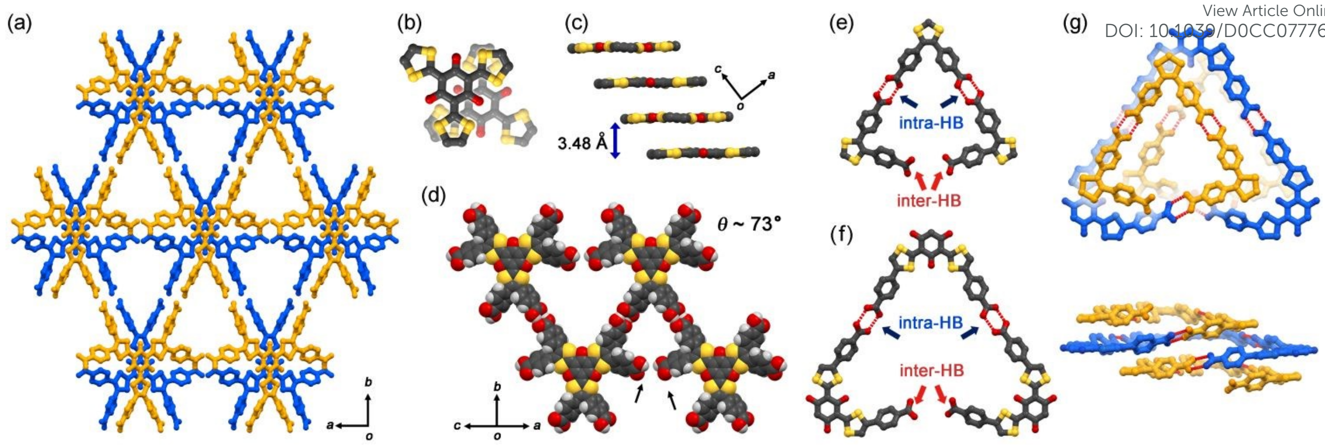

Fig. 2 Crystal structure of **CPDC-1**. (a) Packing diagram, where molecules with diametrically opposed orientation are classified by colours (blue and yellow). (b) Relative orientation of two stacked molecules. (c) Interlayer slipped head-to-tail stacking of **CPDC** molecules viewed along the *b*-axis. (d) Partially H-bonded sheet structure of **CPDC**, where two different partial helical turns (e, f) formed through intralayer H-bonds (intra-HB) connect each other through inter-layer H-bonds (inter-HB) to give anomalous helical motif (g).

Interestingly, four carboxy groups of **CPDC** form intra-layer H-bonds to give a rhombic structural unit, while the other two form inter-layer ones (Fig. 2d). There are two kinds of open-end triangular motif with the different diameters. The motif with a smaller diameter has a pair of phenylene groups appended to the same dithiole ring as a vertex (Fig. 2e), while the one with a larger diameter possesses a pair of phenylene groups appended to the adjacent dithioles as a vertex (Fig. 2f). These two types of motif are connected through interlayer H-bonds to form 3D infinite anomalistic helix along the *c* axis with pitch of 8.6 Å (Fig. 2g). Alternating diameters of helical channel results in shish-kebab-shaped 1D inclusion channel (Fig. S14). The resultant whole framework has ***pcu*** network topology with [$4^{12}.6^3$] point symbol.

The observed H-bonding manner is in contrast to the cyclic and infinite helical motifs observed in **Tp-1** and **CPHAT-1**, respectively (Fig. 1). A closer look at the bite (θ) angles made by the phenylene groups with the π-conjugated central cores reveals a trend in the type of H-bonding motifs formed. The smaller bite angles of 63.2–66.8° in **Tp-1** justify the formation of the discrete cyclic motif akin to an equilateral triangle. On the other hand, a marginal increase to 69.9° enables the H-bonding motif in **CPHAT-1** to form acyclic infinite helical moiety. A further increase in the bite angles to 70.7–72.9°, although trivial, allows **CPDC** to form the complicated helix.

Thermogravimetric analysis of as-formed **CPDC-1** revealed complete desolvation at 585 K, corresponding to a weight loss of 26% (calculated for three MB molecules 26.3%) in two steps (Fig. S15). The first step from 345 to 455 K accounts for the weight loss of one MB molecule, while the second step from 455 to 585 K corresponds to losing of two remaining MB molecules. Further heating leads to rapid weight loss beyond 660 K, which indicates the onset of decomposition. In order to obtain information regarding the structural changes of **CPDC-1** upon heating, variable temperature powder X-ray diffraction (VT-PXRD) patterns were recorded on as-formed crystalline bulks from room temperature to 668 K (Fig. S16). The initial patterns obtained upon heating the bulk crystals are weak until 330 K owing to the severe disorder of solvent molecules in the voids, which is often observed in the case of HOFs.[12] The intensity of the peaks gradually increased while losing the first solvent molecule and hits a plateau at 455 K that continues up to 580 K - the temperature range at which **CPDC-1** loses the two remaining MB molecules to undergo complete desolvation. Subsequently, the intensity dips slightly before peaking at 645 K. Beyond 645 K the intensity starts to descend, indicating the gradual collapse of the H-bonded framework.

Activation of **CPDC-1** was performed by heating the crystals at 473 K for 24 hours under vacuum conditions. Complete removal of the solvent from pores of the crystals and retention of H-bonded framework were evident from the ^{1}H NMR and PXRD patterns, respectively (Figs. S17 and S18). The permanent porosity of **CPDC** obtained upon activation of **CPDC-1** was evaluated by gas adsorption experiments at various temperatures: CO_2 (195 K), N_2 (77 K), O_2 (195 and 77 K), propane (298 K) and propene (298 K) (Fig. S19). The desolvated **CPDC-1** exhibited type-I sorption isotherms for CO_2, propane, and propene, while type-II isotherms for N_2 and O_2. Oxygen uptake at 195 K, 107. 5 kPa was 15.0 cm^3 (0.67 mmol)/g and at 77 K, 20.0 kPa was 10.8 cm^3 (0.48 mmol)/g, while nitrogen at 101.1kPa was 14.6 cm^3 (0.65 mmol)/g. The CO_2 uptake of 67.4 cm^3 (3.01 mmol)/g at 102.3 kPa was highest among the gases used for the experiment, attributed to the smaller kinetic diameter[22] and large quadrupolar moment of CO_2 that leads to increased electrostatic affinity with the aromatic and carbonyl pore surfaces.[23] These results indicate that the HOF has micro pore channels with very small pore width. A comparison of the simulated PXRD pattern obtained from the crystal structure of **CPDC-1** with the PXRD pattern of activated **CPDC-1** reveal marginal shift of the low angle 020 and 110 peaks towards higher 2θ values in the latter, indicating slight shrinkage of the framework upon activation (Fig. S18). The Brunauer–Emmett–

Teller (BET) surface area, $SA_{(BET)}$, calculated based on CO_2 isotherm was 249 $m^2\ g^{-1}$. Furthermore, we carried out propane and propene sorption experiments at room temperature to find out whether the microporous nature of the void can selectively uptake propene over propane. Unfortunately, we could not observe significant difference in sorption volumes of the two, with 21.7 cm^3 (0.97 mmol)/g of propene and 18.9 cm^3 (0.84 mmol)/g of propane being adsorbed at 100.4 kPa.

The crystalline bulk of activated HOF **CPDC-1** exhibited a photocurrent of $\phi\Sigma\mu = 2.8 \times 10^{-5}\ cm^2V^{-1}s^{-1}$ upon exciting at 355 nm as revealed from flash-photolysis time-resolved microwave conductivity (FP-TRMC) measurement (Fig. 3).[24, 25] The observed conductivity in the present DC based HOF is comparable with that obtained in TTF based MOF[26] reported by Dincă's group and could be attributed to the molecular overlap of dithiolylidene rings and close intermolecular S···S contacts. The microcrystalline nature of the sample used for the measurement precluded us from determining the quantum efficiency of the charge carrier generation (ϕ) of **CPDC-1**. Consequently, the charge carrier mobility ($\Sigma\mu$) remains undetermined.

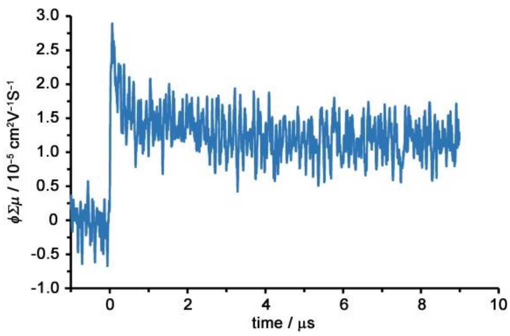

Fig. 3 Transient microwave photoconductivity obtained for the activated **CPDC-1** crystals as revealed from the flash photolysis-TRMC measurement. The excitation wavelength used was 355 nm.

To conclude, by effectively employing the C_3-symmetric tri(dithiolylidene)cyclohexanetrione (DC)-based HOF **CPDC-1**, we have demonstrated the pivotal role of bite angle (θ) on the type of H-bonded motif and network formed. Thanks to five-membered dithiolylidene rings, the larger bite angle in **CPDC** precludes the formation of the frustrated triangular cyclic motif, instead provides an acyclic anomalistic helix with alternating diameters. As a consequence of the H-bonded helical structure, the **CPDC-1** forms a robust 3D, non-interpenetrated network that supports the framework till 645 K. The highly π-delocalised redox core of **CPDC** promotes intermolecular π-stacking and S···S interactions, supporting charge conduction in HOF. Thus, this study offers a promising perspective to tailor the complex topologies and properties of HOFs by bringing subtle geometrical changes in the building blocks.

This work was supported by KAKENHI (JP18H01966 and JP19H04557) and the Dynamic Alliance for Open Innovation Bridging Human, Environment and Materials from MEXT Japan. I.H. thanks Izumi Science and Technology Foundation. K.I.S. thanks RIES, Hokkaido University for financial support. The authors thank Profs. Y. Sagara and N. Tamaoki at RIES, Hokkaido University for purification of compounds by preparative HPLC.

Conflicts of interest

There are no conflicts to declare.

Notes and references

1. Y.-F. Han, Y.-X. Yuan and H.-B. Wang, *Molecules*, 2017, **22**, 266.
2. J. Luo, J.-W. Wang, J.-H. Zhang, S. Lai and D.-C. Zhong, *CrystEngComm*, 2018, **20**, 5884-5898.
3. I. Hisaki, C. Xin, K. Takahashi and T. Nakamura, *Angew. Chem. Int. Ed.*, 2019, **58**, 11160-11170.
4. R.-B. Lin, Y. He, P. Li, H. Wang, W. Zhou and B. Chen, *Chem. Soc. Rev.*, 2019, **48**, 1362-1389.
5. I. Hisaki, *J. Incl. Phenom. Macro.*, 2020, 1-17.
6. B. Wang, R.-B. Lin, Z. Zhang, S. Xiang and B. Chen, *J. Am. Chem. Soc.*, 2020, **142**, 14399-14416.
7. J. Yang, J. Wang, B. Hou, X. Huang, T. Wang, Y. Bao and H. Hao, *Chem. Eng. J.*, 2020, **399**, 125873.
8. M. A. Little and A. I. Cooper, *Adv. Funct. Mat.*, 2020, **30**, 1909842.
9. A. I. Cooper, *ACS Cent. Sci.*, 2017, **3**, 544-553.
10. A. G. Slater and A. I. Cooper, *Science*, 2015, **348**, aaa8075.
11. I. Hisaki, N. Ikenaka, N. Tohnai and M. Miyata, *Chem. Commun.*, 2016, **52**, 300-303.
12. I. Hisaki, S. Nakagawa, N. Ikenaka, Y. Imamura, M. Katouda, M. Tashiro, H. Tsuchida, T. Ogoshi, H. Sato and N. Tohnai, *J. Am. Chem. Soc.*, 2016, **138**, 6617-6628.
13. I. Hisaki, N. Ikenaka, E. Gomez, B. Cohen, N. Tohnai and A. Douhal, *Chem. Eur. J.*, 2017, **23**, 11611-11619.
14. M. Kimura, W. H. Watson and J. Nakayama, *J. Org. Chem.*, 1980, **45**, 3719-3721.
15. I. Hisaki, N. E. Affendy and N. Tohnai, *CrystEngComm*, 2017, **19**, 4892-4898.
16. X. Zheng, N. Xiao, Z. Long, L. Wang, F. Ye, J. Fang, L. Shen and X. Xiao, *Synth. Met.*, 2020, **263**, 116365.
17. Y. Zhang, S. N. Riduan and J. Wang, *Chem. Eur. J*, 2017, **23**, 16419-16431.
18. M. A. Coffin, M. R. Bryce and W. Clegg, *J. Chem. Soc. Chem. Commun.*, 1992, 401-402.
19. K. I. Shivakumar, Goudappagouda, R. G. Gonnade, S. S. Babu and G. J. Sanjayan, *Chem. Commun.*, 2018, **54**, 212-215.
20. J. Nafe and P. Knochel, *Synthesis*, 2016, **48**, 103-114.
21. T. J. Kistenmacher, T. E. Phillips and D. O. Cowan, *Acta Cryst. B*, 1974, **30**, 763-768.
22. D. W. Breck, *Zeolite Molecular Sieves: Structure, Chemistry, and Use* John Wiley and Sons, New York, NY, 1974.
23. I. Hisaki, D. Yasumiya, H. Shigemitsu, S. Tsuzuki, N. Tohnai and M. Miyata, *Phys. Chem. Chem. Phys.*, 2012, **14**, 13918-13921.
24. A. Saeki, Y. Koizumi, T. Aida and S. Seki, *Acc. Chem. Res.*, 2012, **45**, 1193-1202.
25. A. Saeki, *Polym. J.*, 2020, **52**, 1307-1321.

View Article Online
DOI: 10.1039/D0CC07776C

26. T. C. Narayan, T. Miyakai, S. Seki and M. Dincă, *J. Am. Chem. Soc.*, 2012, **134**, 12932-12935.

TOC